

Zero-field Splitting of the Triplet Ground and Excited States of 7H-Benz[de]anthracen-7-ylidene in *n*-Hexane at 1.7 K: A Hole Burning Study

B. Kozankiewicz,* M. Alosyna, and A. Sienkiewicz

Institute of Physics, Polish Academy of Sciences Al. Lotników 32/46, 02-668 Warsaw, Poland

M. Orrit and P. Tamarat

Centre de Physique Moléculaire Optique et Hertzienne, CNRS et Université Bordeaux I, 351 Cours de la Liberation, 33405 Talence Cedex, France

C. M. Hadad, J. R. Snoonian, and M. S. Platz*

Department of Chemistry, The Ohio State University, 100 West 18th Avenue, Columbus, Ohio 43210

Received: December 23, 1999; In Final Form: March 9, 2000

Spectral holes were burned within the inhomogeneous (0,0) fluorescence excitation line of the $T_0 \rightarrow T_1$ transition of 7H-benz[de]anthracen-7-ylidene in an *n*-hexane matrix at 1.7 K. The complicated spectrum of the obtained holes was interpreted with a model taking into account the zero-field splitting (ZFS) of both the triplet states contributing to the transition, the enforced planar symmetry of the carbene, and the domination of internal conversion in the relaxation of the excited T_1 state. Analysis of the hole-burning spectra produced the following ZFS parameters of the ground T_0 and excited T_1 states: $D_0 = (0.274 \pm 0.001) \text{ cm}^{-1} + E_1$, $E_0 = (0.0292 \pm 0.0002) \text{ cm}^{-1} + E_1$ and $D_1 = (0.0168 \pm 0.0002) \text{ cm}^{-1} + E_1$. The number of possible transitions between different spin sublevels is reduced as a consequence of the symmetry plane in the carbene and one of the ZFS parameters, we chose the smallest, E_1 , cannot be estimated. The ZFS parameters of the T_0 state were also estimated by conventional matrix ESR and were in good agreement with the results of the hole burning experiments.

I. Introduction

Carbenes are usually generated by photolysis of diazo, diazirine, and/or ketene precursors with visible or UV light. These molecules are of interest because they contain two nonbonding electrons to distribute into two nonbonding molecular orbitals. Thus, depending on the molecular structure, carbenes may have either a triplet or singlet electronic ground state. Valuable spectroscopic studies have been performed on carbenes immobilized in rigid organic glasses and Shpol'skii matrixes at cryogenic temperatures. These studies include electronic, fluorescence, and magnetic resonance spectroscopy of carbenes which are persistent in the low temperature matrix. This work provides information on the ground state multiplicity of carbenes and their electronic structure. Only carbenes with a triplet ground state (T_0) have been studied to date by fluorescence spectroscopy. In the case of singlet carbenes, the energy separation between the ground and lowest excited singlet states is small, and this favors nonradiative relaxation of the excitation energy.¹

Recently, we have shown^{2–5} that triplet carbenes can be successfully studied by burning holes within the inhomogeneous (0,0) line of the $T_0 \rightarrow T_1$ fluorescence excitation transition. In a low-temperature (1.7 K) Shpol'skii matrix, the $T_0 \rightarrow T_1$ absorption of many carbenes are composed of sharp zero-phonon lines. A slightly different environment of each carbene leads to a distribution of transition energies and the manifold of carbenes creates an inhomogeneous profile of each transition band. The hole-burning technique has been successfully used to separate

a homogeneous component from the inhomogeneously broadened spectrum.⁶

Both triplet states, the T_0 and T_1 , involved in the $T_1 \rightarrow T_0$ transition of triplet carbenes are split into three spin components, in the absence of an external magnetic field.⁷ The hole burning study allowed us to determine this splitting. The zero-field splitting (ZFS) parameter D , which can be extracted from these studies, depends on the spatial distribution of two unpaired electrons, and its value provides important information on the distribution of spin within the triplet carbene. This can explain reactivity differences between the ground and excited states of the carbene.⁸ Furthermore, the number and shape of the holes burned depend on the molecular symmetry of the carbene as well as on the relaxation channels of the excited state.^{2,3}

In this work we present and discuss the results of a hole-burning study of a new, rigid, and planar aromatic carbene, 7H-benz[de]anthracen-7-ylidene (7-BAC). Due to the symmetry plane, the principal spin axis x , perpendicular to the plane, has the same direction in the T_0 and T_1 states. All of the other carbenes studied to date by the hole-burning technique,^{2–4} were lacking in symmetry elements; therefore, the present work provides new information on how the symmetry plane contributes to the shape of burned holes. The spectroscopic characterization of the carbene under investigation can be found in ref 9 and shown in Scheme 1.

II. Experimental Section

7-BAC was obtained in-situ by the photolysis of the 7-diazo-7H-benz[de]anthracene precursor (synthesized in the Columbus Laboratory⁹) dissolved in *n*-hexane at 4.2 K. The precursor concentration was about $2 \times 10^{-3} \text{ mol/L}$. Photolysis was

* Corresponding author E-mail: kozank@ifpan.edu.pl. Fax: (+48-22) 843-0926.

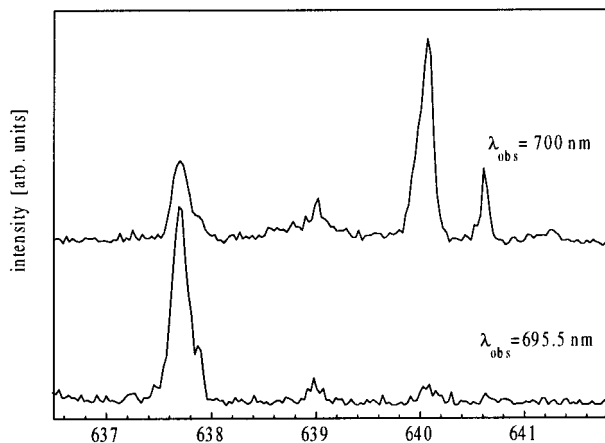
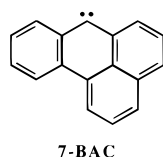


Figure 1. The (0,0) fluorescence excitation inhomogeneous lines of the main sites of 7-BAC in *n*-hexane at 1.8 K.

SCHEME 1



performed with either the 366 or 404 nm line isolated from a mercury lamp. All samples were degassed by the freeze–pump–thaw technique before being inserted into a liquid helium cryostat.

Hole-burning experiments (in the Bordeaux Laboratory) were performed using a single-mode dye laser Coherent, Model No. CR 699-21, having 1–3 MHz frequency resolution and 30 GHz scan width. The lasing dye was Kiton Red. The laser light intensity was stabilized by an electrooptic modulator Conoptics, Model Lass-II. The fluorescence emitted from the sample was collected by an achromatic lens and focused on the slit of a small monochromator. This monochromator was used to select the most intense vibronic lines of carbene, displaced 1315 to 1345 cm^{-1} from the (0,0) origin of the fluorescence. The scattered excitation light was further removed with a RG665 Schott glass filter. Fluorescence intensity was determined in the photon-counting mode by using an RCA photomultiplier, Model No. 31034-A02, cooled to $-20\text{ }^\circ\text{C}$.

Electron spin resonance (ESR) spectra (in the Warsaw Laboratory) were acquired with a Bruker ESP 300 E spectrometer equipped with a standard TE_{102} cavity, Model No. ER 4102 ST (microwave frequency—9.42 GHz). An Oxford Instruments helium gas-flow cryostat, Model No. ESR 910, combined with a Temperature Controller, Model No. ITC 503, allowed the sample temperature to be varied in the 2.7 to 300 K range.

III. Results

7-BAC in an *n*-hexane matrix mainly occupies two sites leading to two (0,0) fluorescence excitation spectra origins with maxima at 640.1 and 637.7 nm^9 and full width at half maximum (fwhm) of 4.6 cm^{-1} , as shown in Figure 1. Hole burning experiments were performed on both of these lines at 1.7 K and typical hole spectra are shown in Figures 2–4.

Within the inhomogeneous (0,0) fluorescence excitation line at 640.1 nm, holes were burned with an intensity of burning light between 1 and 10 mW/cm^2 over a burning time of 100–1000 s. Reading light had usually 10 times lower intensity. The spectrum obtained was composed of several holes located around the central hole, as shown in Figures 2 and 3. The central

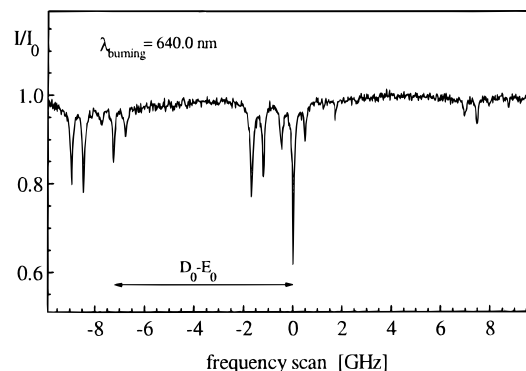


Figure 2. The spectrum of holes burned within the inhomogeneous profile of the (0,0) fluorescence excitation line (having a maximum at 640.1 nm) of 7-BAC in *n*-hexane at 1.7 K. The spectral positions of the holes are given with respect to the frequency of the laser burning light. The presented spectrum was obtained under the following experimental conditions: wavelength of the hole burning light = 640.04 nm, burning intensity = 8 mW/cm^2 , and burning time = 5 min.

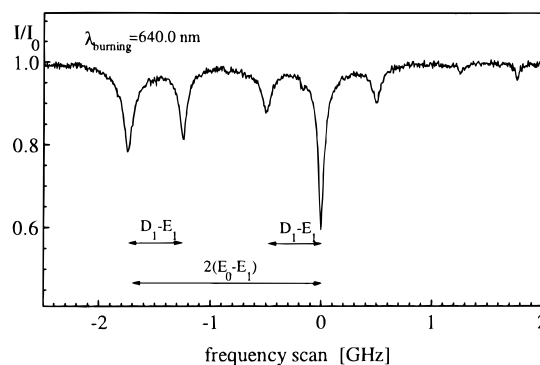


Figure 3. The central part of the spectrum of holes presented in Figure 2.

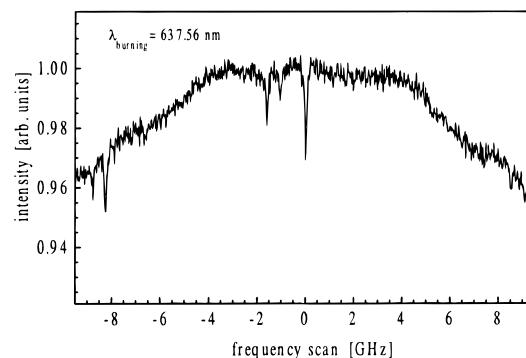


Figure 4. The spectrum of holes burned at the top of the inhomogeneous (0,0) fluorescence excitation line (with a maximum at 637.6 nm) of 7-BAC in *n*-hexane at 1.7 K. The spectral positions of holes are given with respect to the frequency of the laser burning light. The presented spectrum of holes was obtained under the following experimental conditions: wavelength of burning light = 637.6 nm, burning intensity = 80 mW/cm^2 , burning time = 30 min.

hole, at the frequency of the burning laser light, had a fwhm of about 60 MHz and a depth reaching 40%. Several narrow substructures, having fwhm similar to that of the central hole, appeared around this hole in the frequency range between -2 and $+2$ GHz (see Figure 3) and in the broader frequency range between -9 and $+9$ GHz (see Figure 2).

It was much more difficult to burn holes on the second (0,0) fluorescence excitation line at 637.7 nm. We had to use a laser burning intensity as high as 80 mW/cm^2 and a burning time as long as 30 min in order to create the central hole to a depth of

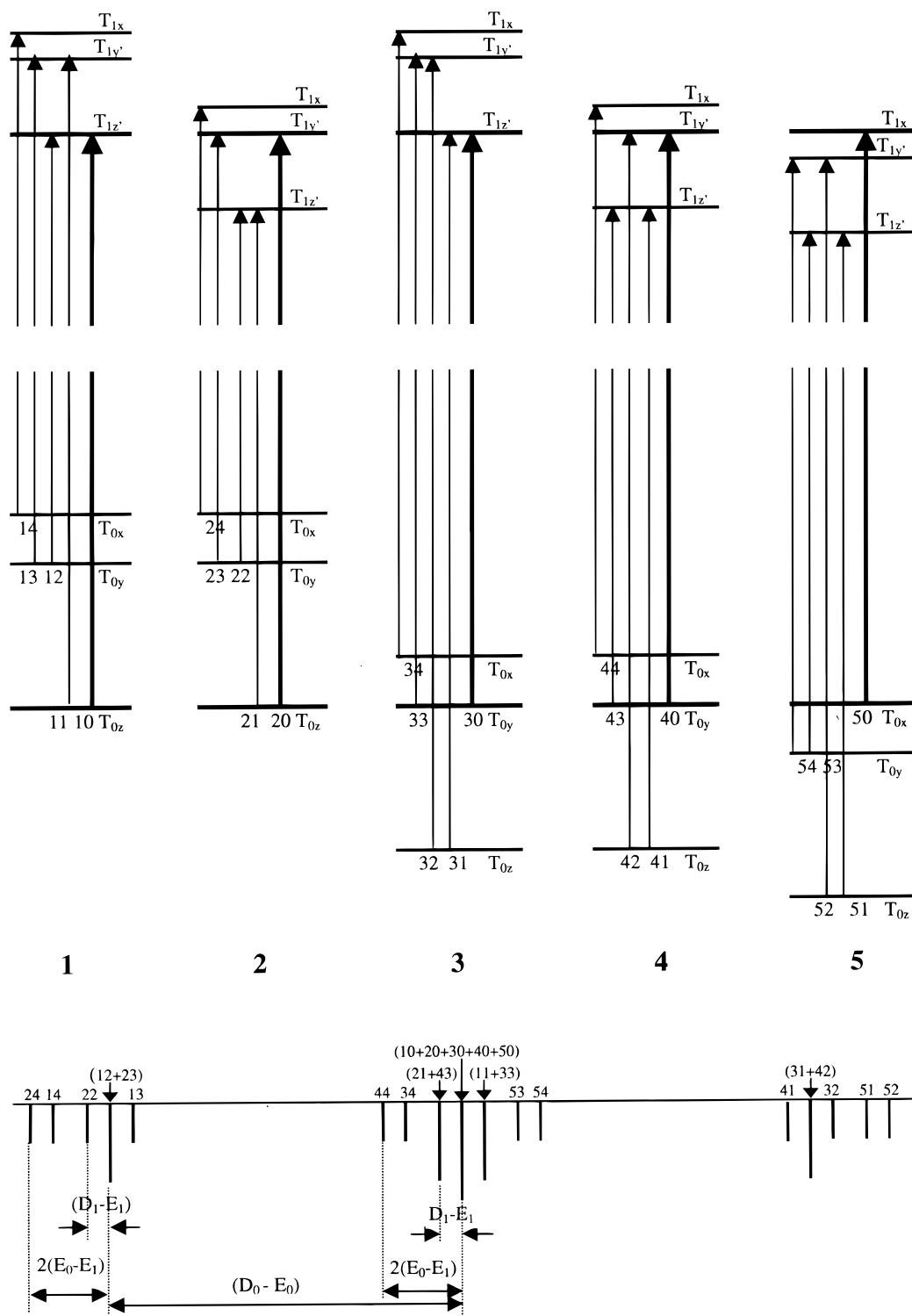


Figure 5. Energy level schemes and absorption transitions of 5 groups of carbenes which can contribute to the observed spectrum of holes. The thick lines indicate the transitions resonant with the frequency of the laser burning light. Predicted spectrum of holes is shown at the bottom of the scheme.

less than 4%. The signal-to-noise ratio was low and only the deepest satellite holes could be identified in the spectrum, as can be seen in Figure 4. The spectral positions of the corresponding holes were slightly different for both sites of the carbene of interest.

IV. Discussion

An energy level scheme which can explain the spectrum of holes detected is presented in Figure 5. Laser light which can

burn holes can be absorbed by 5 groups of carbenes, those that have their $T_{0z} \rightarrow T_{1z'}$, $T_{0z} \rightarrow T_{1y'}$, $T_{0y} \rightarrow T_{1z'}$, $T_{0y} \rightarrow T_{1y'}$ and $T_{0x} \rightarrow T_{1x}$ transitions resonant with the laser light. Those transitions are indicated by thick lines in Figure 5. We used the axes convention proposed by Brandon et al.,¹⁰ where the z axis passes through the central carbene atom and is parallel to the line joining the centers of two adjacent carbon atoms, and the x axis is perpendicular to the plane of the carbene.

Two main considerations were included in the drawing of

the scheme in Figure 5. First, the absorption transition moments are spin-independent; therefore, the absorption rates of different spin sublevels should depend on the projection of the principal spin axes in the ground T_0 state onto the directions of principal spin axes in the T_1 excited state. The 7-BAC carbene contains a symmetry plane and the x direction, perpendicular to that plane, is preserved in the T_0 and T_1 states; whereas the directions z and y in the T_0 can rotate to the new directions z' and y' in the T_1 state. Consequently, the allowed transitions for each carbene are: $T_{0x} \rightarrow T_{1x}$, $T_{0y} \rightarrow T_{1y'}$, $T_{0y} \rightarrow T_{1z'}$, $T_{0z} \rightarrow T_{1z'}$ and $T_{0z} \rightarrow T_{1y'}$.

Furthermore, it is well-known⁵ that there is a much larger separation of the two unpaired electrons in the excited T_1 state than in the ground T_0 state. In the T_0 state, both unpaired electrons are localized close to the central carbene atom (occupying σ and π orbitals); whereas, in the T_1 state, one of those electrons is substantially delocalized onto the aromatic ring (occupying a π^* orbital). Thus, the average separation between unpaired electrons, r , is much larger in the excited state as compared to that in the ground state. The ZFS, in general, includes contributions from both the dipolar spin–spin interaction and the spin–orbit coupling of the two electrons. For triplet carbenes containing only first-row atoms, as in the present example, the spin–orbit contribution is small and the spin–spin interaction dominates.¹¹ Consequently, the ZFS parameter D is proportional to $\langle 1/r^3 \rangle$, and it is much smaller in the excited T_1 than in the ground T_0 state, which simplifies the analysis of the hole spectrum. We can now relate the satellite holes located far away from the central holes (see Figure 2) to the splitting of the T_0 state and the satellite holes located close to the central hole (see Figure 3) to the splitting of the T_1 state.

Spectral positions of the possible absorption transitions (and holes) as well as the energy separations between the main holes are shown at the bottom of Figure 5. Upon comparing the predicted and experimental spectra, we may precisely distinguish and assign all the transitions. The following energy separations (as indicated in Figures 2 and 3) can be directly obtained:

$$2 \cdot (E_0 - E_1) = (1.754 \pm 0.01) \text{ GHz}$$

$$D_1 - E_1 = (0.504 \pm 0.006) \text{ GHz}$$

$$D_0 - E_0 = (7.346 \pm 0.03) \text{ GHz}$$

In this case D_0 and E_0 (and D_1 and E_1) are the ZFS parameters D and E in the ground T_0 (and excited T_1) state, respectively. The above set of three equations contains four independent parameters (D_0 , E_0 , D_1 , and E_1). Therefore, the D_0 , E_0 , and D_1 values can only be obtained with a precision equal to the smallest E_1 value such that:

$$D_0 = (8.223 \pm 0.03) \text{ GHz} + E_1 = \\ (0.274 \pm 0.001) \text{ cm}^{-1} + E_1$$

$$E_0 = (0.877 \pm 0.005) \text{ GHz} + E_1 = \\ (0.0292 \pm 0.0002) \text{ cm}^{-1} + E_1$$

$$D_1 = (0.504 \pm 0.006) \text{ GHz} + E_1 = \\ (0.0168 \pm 0.0002) \text{ cm}^{-1} + E_1$$

The area (and depth) of the holes burned should be dependent on the burning efficiency of the active groups of carbenes as well as on the transition rates between different spin sublevels. A close inspection of the experimental spectra (Figure 2) and the holes predicted from the model (Figure 5) led us to the

following conclusions. The burning efficiency is lower for carbenes from group 5 (burned via the $T_{0x} \rightarrow T_{1x}$ transition) than that of groups 1–4, and that the dominant side holes (numbered by 24, 14, 44, and 34 in Figure 5) correspond to the $T_{0x} \rightarrow T_{1x}$ transitions. We also conclude that the area of these holes can provide information about relative burning efficiency of carbene groups 1–4. Using the area of the $T_{0x} \rightarrow T_{1x}$ hole as an indicator, we find that the burning efficiency of carbene group 1 (burned by the $T_{0z} \rightarrow T_{1z'}$ transition) is slightly larger than that of group 2 (burned by the $T_{0z} \rightarrow T_{1y'}$ transition) and that the burning efficiency of group 4 (burned by the $T_{0y} \rightarrow T_{1y'}$ transition) is slightly larger than that of group 3 (burned by the $T_{0y} \rightarrow T_{1z'}$ transition).

To provide an explanation of these observations, we have to consider a mechanism of burning holes within the profile of the (0,0) fluorescence excitation line of 7-BAC. The 7-BAC carbene seems to be photo stable in low-temperature matrixes because we were able to study samples containing this compound for many days without any detectable drop of fluorescence intensity, as long as the matrix was kept frozen. The hole burning process should therefore proceed via nonradiative relaxation channels, and thus should depend on the amount of relaxation energy dissipated to the neighboring matrix. This relaxation energy can change the carbene-matrix local environment, leading to a new energy minimum. By the same mechanism, a spectral hole is created at the previous position of the zero-phonon line of the carbene which is in resonance with the frequency of the laser burning light. There are two possible channels for nonradiative relaxation of the excitation energy, $T_1 \rightarrow T_0$ internal conversion and $T_1 \rightarrow S_n \rightarrow S_1 \rightarrow T_0$ intersystem crossing. The former process does not differentiate between groups of carbenes. The latter process is known to be highly selective and should strongly favor carbenes from the groups 1 and 2 (which absorb laser light in the T_{0z} spin sublevel), as already observed in the case of 2-naphthylphenylcarbene² and 2,2-dinaphthylcarbene.³ To explain the pattern of holes burned in 7-BAC, we have to assume that the dominant relaxation of the excitation energy in this compound proceeds via the internal conversion channel. Let us add that unlike our previous hole burning studies of 2,2-dinaphthylcarbene,³ we were not able to detect the formation of any anti-holes. The formation of anti-holes requires efficient relaxation by the intersystem crossing pathway, combined with a very long spin–lattice relaxation time in the ground state.

The above conclusion agrees with the analysis of the fluorescence decays.⁹ Upon fitting the fluorescence decays with a three exponential function with the same preexponential factor we found decay time components of 31.2, 42.9, and 43.0 ns.⁹ A slightly shorter decay time component corresponds to the decay rate constant of $3.2 \times 10^7 \text{ s}^{-1}$, the other two, very close to each other, correspond to $2.3 \times 10^7 \text{ s}^{-1}$. Spin–orbit coupling, which is responsible for the intersystem crossing transition ($T_1 \rightarrow S_n$), is usually highly selective, and if this channel operates, one (or two) of the decay rate constants should be much larger than the other two (one). This is not observed for the 7-BAC carbene, where all the component rate constants are similar. We propose that the small ($0.9 \times 10^7 \text{ s}^{-1}$) intersystem crossing contribution is included in the rate constant $3.2 \times 10^7 \text{ s}^{-1}$ and that this slightly enlarged rate describes the energy relaxation of the T_{1x} sublevel. The T_{1x} spin sublevel is therefore partly deactivated by the intersystem crossing pathway, $T_1 \rightarrow S_n \rightarrow S_1 \rightarrow T_0$. It has already been argued in the case of several triplet carbenes^{2,3,12} that the final step in the intersystem crossing pathway, $S_1 \rightarrow T_0$, leads to selective population of the T_{0z} spin

sublevel. If this is the case, then carbenes from group 5, once transferred via intersystem crossing pathway to their T_{0z} sublevel, cannot absorb any new laser photons as long as the spin–lattice relaxation will not transfer these carbenes back to the T_{0x} spin sublevel. The spin–lattice relaxation time is known to be long at 1.7 K;⁵ therefore, the number of photons that can be absorbed by molecules from group 5 should be smaller than those absorbed by the groups of carbenes 1–4. As the burning efficiency depends on the number of photons absorbed, it is reasonable to predict that holes assigned to carbenes from group 5 are much more shallow than those assigned to the four other groups.

To more deeply understand the area (depth) of holes burned, we provide a simple kinetic model. We assumed that the number of molecules burned from group i was given by B_i and that the hole-reading process was described by the expression:

$$A_{nm'} k_r \tau_{m'}$$

where $A_{nm'}$ is the rate constant for the $T_{0n} \rightarrow T_{1m'}$ absorption; k_r is the radiative rate constant, equal for all the spin sublevels of T_1 ; $\tau_{m'}$ is the decay time component of the $T_{1m'}$ sublevel and $\tau_{m'}$ is equal to $1/(k_r + k_{ic} + k_{isc}^{m'})$, where k_{ic} and $k_{isc}^{m'}$ are the rate constants of the internal conversion (equal for all the spin sublevels) and intersystem crossing $T_{1m'} \rightarrow S_j$, respectively. Now the area (and depth) of holes burned can be approximated by the following equations:

$$B_2 \cdot A_{xx} \cdot k_r \cdot \tau_x \approx 23 \quad (1)$$

$$B_1 \cdot A_{xx} \cdot k_r \cdot \tau_x \approx 25 \quad (2)$$

$$B_2 \cdot A_{yz} \cdot k_r \cdot \tau_z \approx 5 \quad (3)$$

$$B_1 \cdot A_{yz} \cdot k_r \cdot \tau_z + B_2 \cdot A_{yy} \cdot k_r \cdot \tau_y \approx 16 \quad (4)$$

$$B_1 \cdot A_{yy} \cdot k_r \cdot \tau_y \approx 9 \quad (5)$$

$$B_4 \cdot A_{xx} \cdot k_r \cdot \tau_x \approx 26 \quad (6)$$

$$B_3 \cdot A_{xx} \cdot k_r \cdot \tau_x \approx 22 \quad (7)$$

$$B_2 \cdot A_{zz} \cdot k_r \cdot \tau_z + B_4 \cdot A_{yz} \cdot k_r \cdot \tau_z \approx 17 \quad (8)$$

$$B_1 \cdot A_{zz} \cdot k_r \cdot \tau_z + B_2 \cdot A_{zy} \cdot k_r \cdot \tau_y + B_3 \cdot A_{yz} \cdot k_r \cdot \tau_z + B_4 \cdot A_{yy} \cdot k_r \cdot \tau_y + B_5 \cdot A_{xx} \cdot k_r \cdot \tau_x \approx 54 \quad (9)$$

$$B_1 \cdot A_{zy} \cdot k_r \cdot \tau_y + B_3 \cdot A_{yy} \cdot k_r \cdot \tau_y \approx 14 \quad (10)$$

$$B_5 \cdot A_{yz} \cdot k_r \cdot \tau_z \approx 3 \quad (11)$$

$$B_5 \cdot A_{yy} \cdot k_r \cdot \tau_y \approx 5 \quad (12)$$

$$B_4 \cdot A_{zz} \cdot k_r \cdot \tau_z \approx 8 \quad (13)$$

$$B_3 \cdot A_{zz} \cdot k_r \cdot \tau_z + B_4 \cdot A_{zy} \cdot k_r \cdot \tau_y \approx 11 \quad (14)$$

$$B_3 \cdot A_{zy} \cdot k_r \cdot \tau_y \approx 2 \quad (15)$$

$$B_5 \cdot A_{zz} \cdot k_r \cdot \tau_z \approx 4 \quad (16)$$

$$B_5 \cdot A_{zy} \cdot k_r \cdot \tau_y \approx 2 \quad (17)$$

The relative area of holes burned (estimated from the experimental holes and given on the right side of the above equations) differ in different spectra (within the range of 20% for the deepest holes), and therefore, the values of estimated rate constants are the subject of high experimental error. We should also warn the reader that the observed holes are deep and therefore may have been obtained at the fluence saturation

condition. To avoid this problem the relative area of holes as a function of burning fluence would have to be studied and next, the results would have to be extrapolated to zero fluence. Another source of experimental error may be due to optical pumping to different spin sublevels of the T_0 state in connection with a long spin–lattice relaxation time at 1.7 K.

Using the eqs 1, 2, 6, and 7 we can easily estimate that $B_1:B_2:B_3:B_4 \approx 23:25:26:22$. Using the eqs 5 and 12 we estimate that $B_1:B_5 \approx 9:5$, and thus we can find the relative number of burned molecules from each group of carbenes.

From eq 4/eq 5 we can obtain $A_{yz} \cdot t_z = 0.85 A_{yy} \cdot t_y$ and from eq 14/eq 13 that $A_{zy} \cdot t_y = 0.53 A_{zz} \cdot t_z$. We assumed further that $\tau_z = \tau_{y'}$, which was already postulated, and that $A_{ij'} = A \cdot \langle S_i | S_j \rangle^2$, where S_i and S_j are spin wave functions of the i and j' spin sublevels in the ground and excited triplet states, respectively. We easily found that $\langle S_y | S_y \rangle^2 = 0.54$ and $\langle S_z | S_z \rangle^2 = 0.65$ and hence, the angle between the principal spin axes y and y' was found to be 42° and between the axes z and z' was 36° . The principal spin axes y , z , and y' , z' are located on the same plane of carbene; therefore, we expect that both spin axes should rotate by the same angle. Some small difference (42° as compared with 36°) is due to assumptions used previously to derive the formulas and to the experimental error in the determination of the areas of the holes.

A detailed kinetic analysis is much more difficult for the second carbene site, with a (0,0) band maximum at 637.7 nm. The spectral positions of holes presented in Figure 4 allowed us to estimate that:

$$D_0 = (8.085 \pm 0.03) \text{ GHz} + E_1 = (0.270 \pm 0.001) \text{ cm}^{-1} + E_1$$

$$E_0 = (0.80 \pm 0.03) \text{ GHz} + E_1 = (0.027 \pm 0.001) \text{ cm}^{-1} + E_1$$

$$D_1 = (0.54 \pm 0.02) \text{ GHz} + E_1 = (0.018 \pm 0.0005) \text{ cm}^{-1} + E_1$$

The ZFS parameters, obtained for both sites of 7-BAC in n -hexane are similar, indicating that a matrix contribution to the spin distribution is small. Nevertheless, the burning efficiency in both insertion sites was very much different. We can speculate that 7-BAC molecules in the 637.7 nm site are well packed between the parallel chains of the n -hexane matrix, whereas the 640.1 nm site provides more space for carbene reorientation.

Conventional electron spin resonance (ESR) has been successfully used to determine the ZFS parameters of many triplet carbenes.¹³ We used this technique to compare the ZFS parameters of the ground triplet state obtained from ESR studies with those obtained using the hole-burning approach. The conventional ESR spectrum that was obtained is shown in Figure 6. The experimental conditions were as close as possible to that employed during our hole-burning experiments, despite the different technical requirements of both techniques. The diazo precursor concentration was about 2×10^{-3} mol/L (close to the experimental low concentration limit required in ESR experiments) and the experiment was performed in a polycrystalline matrix of n -hexane at 3.5 K. The spectrum was composed of several sharp lines. We identified and assigned, according to ref 14, the following lines as the resonance field positions of 7-BAC: z_1 (497 and 529 G, probably corresponding to two sites of the carbene), x_2 (4236 G), y_2 (4878 G), and z_2 (6171 G). The resonance field of 3362 G corresponds to a free radical impurity

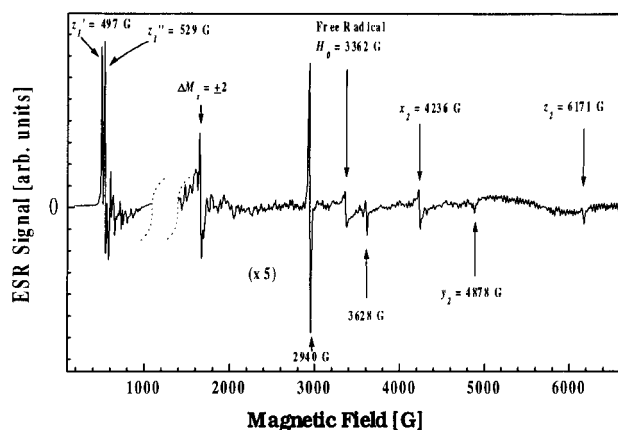


Figure 6. ESR spectrum of 7-BAC in *n*-hexane at 3.5 K. The arrows indicate resonance field positions assigned to the z_1 , x_2 , y_2 , and z_2 components of the carbene's spectrum. z_1' and z_1'' lines are assigned to two different sites of 7-BAC.

and the resonance at 1654 G is the half-field, $\Delta M_s = \pm 2$, transition of the triplet carbene. Strong lines at 2940 and 3628 G disappeared with an increase in temperature much faster than the lines assigned to the carbene indicating their different origin. We are not able at present to provide the origin of these lines. Using the well-known procedure,¹⁴ and assuming that the g tensor values are independent of direction, we found that $D_0 = 0.265 \pm 0.004 \text{ cm}^{-1}$ and that $E_0 = 0.017 \pm 0.002 \text{ cm}^{-1}$. The ZFS parameters obtained by the ESR technique are very close to, but slightly smaller than, the values obtained from the hole-burning experiment. The origin of this small discrepancy may be due to a weak direction dependence of the g tensor.

V. Conclusion

In this work we present and discuss the first successful hole burning within the inhomogeneous profile of the (0,0) fluorescence excitation line of planar 7H-benz[de]anthracen-7-ylidene (7-BAC) in an *n*-hexane matrix at 1.7 K.

Absorption transition moments are spin-independent; therefore, the transitions from different spin sublevels of the triplet ground-state T_0 to spin sublevels of the excited T_1 state depend on the projection of the corresponding principal spin axes. In 7-BAC, the principal spin axis x , perpendicular to the symmetry plane of carbene, is preserved in the T_0 and T_1 states; whereas the axes z and y can rotate to new z' and y' . Consequently, the only transitions allowed are: $T_{0x} \rightarrow T_{1x}$, $T_{0y} \rightarrow T_{1y}$, $T_{0y} \rightarrow T_{1z'}$, $T_{0z} \rightarrow T_{1z'}$, and $T_{0z} \rightarrow T_{1y'}$. To explain the spectrum of holes observed, we had to assume that the dominant relaxation channel of the excitation energy present in the T_1 state proceeded via internal conversion.

Analysis of the frequency positions of satellite holes directly provided the ZFS parameters of the T_0 and T_1 states: $D_0 = (0.274 \pm 0.001) \text{ cm}^{-1} + E_1$, $E_0 = (0.0292 \pm 0.0002) \text{ cm}^{-1} + E_1$, and $D_1 = (0.0168 \pm 0.0002) \text{ cm}^{-1} + E_1$. The inability to estimate one of the ZFS parameters, E_1 , is a consequence of a

symmetry plane in the carbenes which reduced the number of possible transitions between different spin sublevels (and thus holes). The ZFS parameters of carbenes located in the other site of the Shpol'skii matrix of *n*-hexane are slightly different: $D_0 = (0.270 \pm 0.001) \text{ cm}^{-1} + E_1$, $E_0 = (0.027 \pm 0.001) \text{ cm}^{-1} + E_1$, and $D_1 = (0.018 \pm 0.0005) \text{ cm}^{-1} + E_1$. A conventional ESR experiment, performed at conditions close to those utilized during hole burning, provided ZFS parameters of the triplet ground state which are similar to the values obtained by the hole burning method. This establishes the complementarity of the two experimental techniques.

The areas of the holes burned depend on the burning efficiency of different groups of carbenes as well as on transition rates characterizing different spin sublevels. The most interesting result of the simple kinetic model, used to relate the areas of the satellite holes burned, is that the principal spin axes z and y in the T_0 state rotate by about 40° (in the symmetry plane of carbene) to their new corresponding positions z' and y' in the excited T_1 state.

Acknowledgment. B.K. is indebted to the University of Bordeaux for a visiting professor fellowship. Support of this work in Columbus by the National Science Foundation is greatly acknowledged by M.S.P. (CHE-9613861) and C.M.H. (CHE-9733457). J.R.S. greatly acknowledges support by an OSU postdoctoral fellowship. A.S. acknowledges support by the Polish KBN Grant #2-PO3B-018-13.

References and Notes

- (1) (a) Sander, W.; Bucher, G.; Wierlacher, S. *Chem. Rev.* **1993**, *93*, 1583. (b) Shpol'skii, E. V.; Iliina, A. A.; Klimova, L. A. *Dokl. Acad. Nauk. USSR* **1952**, *87*, 935. (c) Trozzolo, A. M. *Acc. Chem. Res.* **1968**, *1*, 329. (d) Pliego, J. R., Jr.; De Almeida, W. B.; Celebi, S.; Zhu, Z.; Platz, M. S. *J. Phys. Chem. A* **1999**, *103*, 7481.
- (2) Kozankiewicz, B.; Bernard, J.; Migirdicyan, E.; Orrit M.; Platz, M. S. *Chem. Phys. Lett.* **1995**, *245*, 549.
- (3) Kozankiewicz, B.; Aleshyna, M.; Gudmundsdottir, A. D.; Platz, M. S.; Orrit M.; Tamarat, Ph. *J. Phys. Chem. A* **1999**, *103*, 3155.
- (4) Kozankiewicz, B.; Bernard, J.; Migirdicyan, E.; Orrit M.; Platz, M. S. *Mol. Cryst. Liq. Cryst.* **1996**, *283*, 191; **1996**, *291*, 143.
- (5) Migirdicyan, E.; Kozankiewicz B.; Platz, M. S. In *Advances in Carbene Chemistry*; Brinker, U., Ed.; JAI Press Inc.; Stamford, CT, 1998; Vol. 2, p 97.
- (6) Personov, R. I. In *Spectroscopy and Excitation Dynamics of Condensed Molecular Systems*; Agranovich, V. M.; Hochstrasser, R. M., Eds.; North-Holland: Amsterdam, 1983; p 555.
- (7) McGlynn, S. P.; Azumi, T.; Kinoshita, M. *Molecular Spectroscopy of the Triplet State*; Prentice-Hall: Englewood Cliffs, NJ, 1969.
- (8) Turro, N. J.; Aikawa, M.; Butcher, J. A., Jr.; Griffin, G. W. *J. Am. Chem. Soc.* **1980**, *102*, 5127.
- (9) Aleshyna, M.; Kozankiewicz, B.; Hadad, C. M.; Snoonian J.; Platz, M. S. *J. Phys. Chem. A* **2000**, *104*, 3391.
- (10) Brandon, W. R.; Closs G. L.; Hutchison C. A., Jr. *J. Chem. Phys.* **1962**, *37*, 1878.
- (11) Hutton R. S.; Roth, H. D. *J. Am. Chem. Soc.* **1982**, *104*, 7395.
- (12) Doetschman, D. C.; Botter, B. J.; Schmidt J.; van der Waals, J. H. *Chem. Phys. Lett.* **1976**, *38*, 18.
- (13) Trozzolo, A. M.; Wasserman, E. In *Carbenes*; Moss, R. A., Jones, M., Jr., Eds.; Wiley: New York, 1975, Vol. II, p 185.
- (14) Wasserman, E.; Snyder L. C.; Yager, W. A. *J. Chem. Phys.* **1964**, *41*, 1763.